



## PERFORMANCE-BASED SEISMIC DESIGN USING AN INTEGRATED STRUCTURAL RELIABILITY EVALUATION APPROACH

J.R. Gaxiola-Camacho <sup>(1)</sup>, A. Haldar <sup>(2)</sup>, F.J. Villegas-Mercado <sup>(3)</sup>, A. Reyes-Salazar <sup>(4)</sup>

<sup>(1)</sup> PhD Candidate, The University of Arizona, jrgaxiola@email.arizona.edu

<sup>(2)</sup> Professor, The University of Arizona, haldar@email.arizona.edu

<sup>(3)</sup> PhD Student, The University of Arizona, fcovillegas@email.arizona.edu

<sup>(4)</sup> Professor, Universidad Autónoma de Sinaloa, reyes@uas.edu.mx

### Abstract

The Performance-Based Seismic Design (PBSD) requirements, now under development, are expected to be incorporated in the next generation of design guidelines. Considering the economic impacts of recent major earthquakes all over the world, the PBSD guidelines need to be developed as expeditiously as possible. Since PBSD is a risk-based concept, an appropriate risk evaluation procedure must be available that will satisfy all the concerned parties. To satisfy the deterministic design community and all implicated authorities who make the final decision, the practices generally applied need to be followed. Structures must be represented by finite elements and the seismic loading has to be applied in time domain incorporating all major sources of nonlinearity. Then, the information on uncertainty needs to be incorporated in the formulation. However, for the class of problems under consideration, the required Limit Performance Functions (LPFs) become implicit. Besides the basic Monte Carlo Simulation (MCS) method, the authors believe no other suitable reliability analysis procedure is currently available. A novel reliability evaluation procedure is proposed to fill this knowledge gap. The basic response surface method is significantly improved by removing its three major deficiencies and then it is integrated with the First-Order Reliability Method (FORM) to locate the failure region. In this way, an implicit LPF is approximately represented by a second order polynomial. Then, FORM is used to extract the reliability information. The authors developed required serviceability and strength LPFs and correlated them with the three performance levels of Collapse Prevention (CP), Life Safety (LS), and Immediate Occupancy (IO), as suggested by FEMA and SAC. The proposed method is further illustrated with the help of an example. A 3-story steel frame, designed by experts satisfying post-Northridge design requirements, as reported by FEMA, is considered for this purpose. The structure is excited by three sets of ground motions representing three performance levels of CP, LS, and IO. Each set contains 20 time histories representing one specific performance level. For the serviceability LPFs, performance requirements suggested by FEMA and SAC are evaluated. The results indicate that the design guidelines suggested by them are very appropriate. They are very similar to the values reported in the currently used Load and Resistance Factor Design (LRFD) guidelines. For the strength LPFs, the authors assumed that the performance requirements for serviceability LPFs would also be applicable to strength LPFs. They used the interaction equations suggested in the AISC design manuals. The authors observed that the seismic design of structures needs to be performed by using several earthquake time histories, as suggested in some recent design guidelines. The reliability indexes estimated with the proposed method correlate well with different levels of performance indicating that the proposed reliability method is viable. The results and observations made in this study clearly indicate that the reliability information can be obtained using only few hundreds instead of several thousands or millions of deterministic analyses. The authors very strongly believe that the proposed reliability evaluation method can be used to advance in the development of the PBSD concept.

*Keywords: Performance-based seismic design; finite element method; first-order reliability method; response surface method; limit performance functions.*

### 1. Introduction

The Performance-Based Seismic Design (PBSD) concept is an attractive alternative in developing the next generation of design guidelines or nonprescriptive codes. It provides an option to the owner of a structure to select the current design practice of life safety or its alternative of limiting property damage or loss of economic activities. The later alternative has attracted serious attention from the profession due to severe economic impact caused by several recent earthquakes all over the world. In a comprehensive study funded by the Federal



Emergency Management Agency (FEMA), the PBSD concept was advocated in several reports including FEMA-273 [1] and SAC [a joint venture of the Structural Engineers Association of California (SEAOC), Applied Technology Council (ATC), and California Universities for Research in Earthquake Engineering (CUREE)] [2-4]. The primary objective of the PBSD concept is to design structures for different performance levels satisfying some prescribed risks. Obviously, different risk levels will have different consequences and the owner or the responsible parties are willing to accept such outcomes reflecting their preferences. One of the major challenges in developing the PBSD guidelines is the estimation of risk corresponding to different performance levels acceptable to all concerned parties. The authors believe that no such risk evaluation procedure is currently available. It is essential at this time to fill this knowledge gap before moving forward with the PBSD guidelines.

## 2. Literature review

The novel concept behind the PBSD guidelines is still being developed and the available literature on the topic is very limited. In developing the concept, FEMA 355F [4] identified six items that need to be addressed in developing the guidelines. They are: (1) account for uncertainty in the performance associated with unanticipated events, (2) set realistic expectations for performance, (3) assess performance variables in similar buildings located nearby, (4) develop a reliability framework, (5) set representative performance levels for various seismic hazards, and (6) quantify local and global structural behaviors leading to collapse. There is a knowledge gap specifically in addressing item (4). The SAC project [2-4] suggested a reliability framework but failed to identify any appropriate procedure acceptable to all parties. Based on a comprehensive literature review, the authors concluded that the currently available reliability evaluation procedures cannot be used to implement the PBSD guidelines, and a new procedure needs to be developed as expeditiously as possible. In developing such a novel reliability evaluation approach, it should be noted that the design community, in general, is not familiar with the reliability-based concept. However, since they make the final design decision, their interests or concerns must be taken into account.

To satisfy the needs of the deterministic design community, the authors decided to incorporate several features routinely used by them. Risk is always estimated with respect to a specific Limit Performance Function (LPF). In estimating the probability of failure ( $p_f$ ), it is necessary to follow the same failure path used by the deterministic community, i.e., structural performance should be tracked from elastic, to inelastic, and to complete collapse. Before failure, the structure develops several sources of nonlinearities. To incorporate all these features, the engineering profession represents the structures by finite elements. Thus, it is essential that the proposed reliability evaluation technique should also be finite element-based. In the most sophisticated deterministic seismic response analysis, the seismic loading is applied in time domain. In any new reliability evaluation procedure, the seismic loading also needs to be applied in time domain. In summary, the reliability evaluation procedure should be finite element-based, the seismic loading needs to be applied in time domain, and capable of estimating risk in the presence of all major sources of nonlinearity and uncertainty. These requirements or expectations make the risk evaluation very challenging.

As mentioned earlier, for nonlinear structures excited by seismic loading in time domain, the required LPFs become implicit in nature. Since the calculation of derivatives of the LPFs with respect to the design variables becomes extremely tedious [5], the risk estimation by commonly used First-Order or Second-Order Reliability Method (FORM/SORM) is very demanding. When LPFs are implicit, among several options, the basic Monte Carlo Simulation (MCS) becomes an attractive alternative. The basic MCS procedure is relatively simple to implement but is not efficient. It requires thousands or millions of deterministic analyses for extracting reliability information, requiring several thousands of hours of computational time. As an alternative to basic MCS, the Response Surface Method (RSM) can also be used to approximately generate a LPF of interest. In the context of RSM, several deterministic evaluations are conducted following a sampling scheme around a center point to generate the response information. Then, a polynomial is used to fit the response data, sometimes using regression analysis. However, the basic commonly used RSM procedure has three major deficiencies: it cannot incorporate information on the distribution of Random Variables (RVs) even when it is available, if the seismic responses are not obtained in the failure region (it is unknown for most problems of interest), the extracted reliability information will be unacceptable, and the required optimal sampling scheme for accurate generation of a Response Surface (RS) is an open question. In order to address the first two deficiencies, the authors



propose to integrate RSM and FORM. The iterative process of FORM will incorporate the distributional information of RVs and it will locate the Most Probable Failure Point (MPFP). For the third deficiency, the authors suggest an advanced reliability scheme for sampling point selection. Hence, an accurate RS can be generated to represent a LPF. Once the explicit expression of a RS is obtained, FORM can be used to estimate the underlying risk.

### 3. An integrated structural reliability evaluation approach

Based on the above discussions, it is necessary at this time to develop a reliability evaluation procedure by representing a structure using finite elements, and exciting it by seismic loading applied in time domain considering all major sources of nonlinearity and uncertainty. A novel concept is proposed in this paper and systematically presented in the following sections.

#### 3.1 Finite element evaluation

An essential part of the proposed method is representing a structure to be designed by the PBSD concept using finite elements (FEs). Considering its numerous advantages over the commonly used displacement-based finite element method, the Stress-Based FE Method (SB-FEM) is selected in this study for the calculation of deterministic seismic responses [6]. There are several attractive features of SB-FEM, particularly when a structure is of frame type. The tangent stiffness matrix can be expressed in an explicit form, requiring fewer elements for the FE analysis. Using SB-FEM, numerical integration is not necessary for the calculation of the stiffness matrix at each step of time domain analysis. A comprehensive description of SB-FEM is beyond the scope of this paper. The research team at the University of Arizona has extensively developed and verified the SB-FEM procedure. It is widely available in the literature [7-10]. The team also developed a sophisticated computer program. It is extensively used in developing the novel PBSD concept.

#### 3.2 Integration process of RSM and FORM

In order to accurately generate a RS, distributional information of RVs and the failure region need to be considered. As discussed earlier, the authors decided to integrate RSM and FORM to incorporate the above information in the formulation. Using the basic RSM concept to generate a RS [11], the center point, sampling points, and sampling region are selected as:

$$X_i = X_i^C + hx_i\sigma_{X_i} \quad \text{where } i = 1, 2, \dots, k \quad (1)$$

where  $k$  is the number of RVs,  $X_i$  is the region or bound of the  $i^{\text{th}}$  RV,  $X_i^C$  is the coordinate of the center point of the  $i^{\text{th}}$  RV,  $h$  is an arbitrary factor controlling the experimental sampling region,  $x_i$  is the coded variable which has values of 0,  $\pm 1$ , or  $\sqrt[4]{2^k}$ , and  $\sigma_{X_i}$  is the standard deviation of the  $i^{\text{th}}$  RV. The formulation represented by Eq. (1) does not incorporate distributional information of RVs, and selection of the simulation or failure region is subjective. In the integrated process of RSM and FORM, the underlying distribution of RVs will be incorporated through the FORM iterations. It is widely known that FORM is used in the normal variable space. However, for the reliability evaluation of real structures of interest, all RVs are not expected to be normal. In the context of FORM, all non-normal RVs need to be transformed to equivalent normal RVs at the checking point. The equivalent standard deviation ( $\sigma_{X_i}^N$ ) and mean ( $\mu_{X_i}^N$ ) can be calculated by equating the Cumulative Distribution Functions (CDFs) and the Probability Density Functions (PDFs) of the original non-normal RVs to those of the equivalent normal variables [5] as:

$$\sigma_{X_i}^N = \frac{\Phi\{\Phi^{-1}[F_{X_i}(x_i^*)]\}}{f_{X_i}(x_i^*)} \quad (2)$$

and

$$\mu_{X_i}^N = x_i^* - \Phi^{-1}[F_{X_i}(x_i^*)]\sigma_{X_i}^N \quad (3)$$



where  $\Phi(\cdot)$  and  $\phi(\cdot)$  are the CDF and PDF of the standard normal variable, respectively,  $x_i^*$  is the checking point, and  $F_{X_i}(x_i^*)$  and  $f_{X_i}(x_i^*)$  represent the CDF and PDF of the original non-normal variables at the checking point  $x_i^*$ , respectively. Once all the non-normal RVs are transformed to equivalent normal variables, the iteration process of FORM will be initiated by substituting  $X_i$  and  $\sigma_{X_i}$  in Eq. (1) by  $\mu_{X_i}^N$  and  $\sigma_{X_i}^N$ , respectively.

### 3.3 Explicit representation of response surface

In the context of PBSO, the explicit mathematical form of a RS is expected to be nonlinear. The selection of more than second order polynomials for a RS may result in ill-condition of the system of equations, complicating the process [11]. Hence, the authors propose to mathematically represent a RS using a second-order polynomial without or with cross terms. They can be represented as:

$$\hat{g}(\mathbf{X}) = b_0 + \sum_{i=1}^k b_i X_i + \sum_{i=1}^k b_{ii} X_i^2 \quad (4)$$

and

$$\hat{g}(\mathbf{X}) = b_0 + \sum_{i=1}^k b_i X_i + \sum_{i=1}^k b_{ii} X_i^2 + \sum_{i=1}^{k-1} \sum_{j>1}^k b_{ij} X_i X_j \quad (5)$$

where  $X_i$  ( $i=1,2,\dots,k$ ) is the  $i^{\text{th}}$  RV,  $k$  was defined earlier,  $b_0$ ,  $b_i$ ,  $b_{ii}$  and  $b_{ij}$  are the unknown coefficients to be determined, and  $\hat{g}(\mathbf{X})$  is the approximate explicit expression for the RS of interest, representing the original unknown RS [ $g(\mathbf{X})$ ]. The numbers of unknown coefficients to be estimated in the above two equations play a very important role in the efficiency and accuracy of the integrated approach. If Eq. (4) is used, the number of coefficients to be determined will be  $2k + 1$ . If Eq. (5) is used, it will be  $(k + 1)(k + 2)/2$ . Obtaining an optimal number of coefficients to be used in generating a RS is one of the objectives of this study. It mainly depends on the number of RVs present in defining a LPF and performance level under consideration. This will be discussed in more detail later.

### 3.4 Advanced reliability scheme for the selection of experimental sampling points to generate a response surface

The efficiency and accuracy of the integrated approach will mainly depend on the selection of the experimental sampling points around a center point. This will be denoted as the Total Number of Sampling Points (TNSP) or deterministic FE analyses required to generate a RS. In the context of FORM, the iteration process will be initiated at the mean values of all RVs and it will be the initial center point. Two commonly used schemes for selecting experimental sampling points are Saturated Design (SD) and Central Composite Design (CCD) [11]. In SD, a second-order polynomial without [Eq. (4)] or with [Eq. (5)] cross terms can be utilized and the required RS can be generated by solving a set of equations. SD requires only as many TNSP as the total number of unknown coefficients of the RS. The TNSP required to generate a RS without and with cross terms using SD can be shown to be  $2k + 1$  and  $(k + 1)(k + 2)/2$ , respectively. SD is expected to be very efficient, but its accuracy cannot be assured. CCD is expected to be very accurate but inefficient. It requires a second-order polynomial with cross terms [Eq. (5)] and a regression analysis if required to generate a RS. The TNSP required to implement CCD with a second-order polynomial with cross terms will be  $2^k + 2k + 1$ . Suppose that the reliability of a structure will be obtained by considering 70 RVs ( $k = 70$ ). The TNSP required using SD without and with cross terms will be 141 and 2556, respectively. But for CCD, it will require  $1.180591621 \times 10^{21}$  TNSP. The above discussion clearly indicates the implications of using different sampling schemes.

When  $k$  is large, it is impractical to use CCD. To retain accuracy, the authors propose to reduce the total number of RVs present in a LPF using the sensitivity analysis as suggested by Haldar and Mahadevan [5]. The sensitivity index can be defined in terms of direction cosines of RVs, readily available from the FORM analysis. RVs with low sensitivity indexes can be treated as deterministic at their mean values in subsequent iterations.



The reduced number of RVs is denoted hereafter as  $k_r$ . Suppose, out of a total of 70 RVs, only 7 are found to be very sensitive, i.e.,  $k_r = 7$ . TNSP required to implement CCD will be  $2^7 + 2 * 7 + 1 = 143$ . The authors observed that the efficiency of the proposed algorithm can be significantly improved without compromising accuracy by reducing the total number of RVs in a formulation. Based on this discussion, the authors proposed the following Advanced Reliability Scheme (ARS). In the first iteration, a required RS will be generated using SD without cross terms. Then, using FORM, the direction cosines of all RVs will be estimated. Using the information, only  $k_r$  number of RVs will be used in all subsequent iterations. In order to locate the MPFP, several iterations may be required. For these intermediate iterations, SD without cross terms [Eq. (4)] can be used but with  $k_r$  number of RVs. Then, in the last iteration, CCD with cross terms [Eq. (5)] will be used to extract the reliability information. Suppose, the reliability of a structure needs to be estimated for a LPF with  $k = 70$ . Only 7 RVs are found to be the most sensitive, thus,  $k_r = 7$ . TNSPs required to implement the proposed procedure can be shown to be  $(2 * k + 1) + (2 * k_r + 1) + (2^{k_r} + 2 * k_r + 1) = (2 * 70 + 1) + (2 * 7 + 1) + (2^7 + 2 * 7 + 1) = 299$ . The authors believe that this is very reasonable as compared to thousands or millions of MCS.

### 3.5 Evaluation of performance levels

The generation of required LPFs will be the next important step. At this time, the information on RSs is available. The information can be used to generate required LPFs if performance levels are known. FEMA 350 [2] defined three performance levels: Immediate Occupancy (IO), Life Safety (LS), and Collapse Prevention (CP). Since PBSD is implemented in terms of multiple target performance levels, FEMA-273 [1] and -350 [2] suggested allowable drift values ( $\delta_{allow}$ ) for the CP, LS, and IO performance levels in terms of earthquake return period and probability of exceedance. They are summarized in Table 1.

Table 1 – Allowable drifts corresponding to CP, LS, and IO performance levels for different seismic hazards.

Performance Level	Earthquake Return Period	Probability of Exceedance	Allowable Drift ( $\delta_{allow}$ )
CP	2475-year	2% in 50 years	$0.050 * H$
LS	475-year	10% in 50 years	$0.025 * H$
IO	72-year	50% in 50 years	$0.007 * H$

In Table 1,  $\delta_{allow}$  is a function of  $H$ . It represents the total height of the structure under consideration if overall top roof drift is evaluated, or the story height if inter-story drift is considered. The information provided in Table 1 is essentially for serviceability LPFs. Due to lack of any information, the authors assumed that the same performance requirements would also be applicable to the strength LPFs. For the generation of strength LPFs, the authors used the interaction equations suggested by the American Institute of Steel Construction (AISC) [12]. Considering that a structure may fail due to excessive lateral deflection or failure of several members due to a major seismic excitation, the authors believe that both serviceability and strength LPFs need to be considered separately in developing the PBSD guidelines.

#### 3.5.1 Serviceability LPF

For seismic loading, the serviceability LPF can be generally expressed as:

$$g(\mathbf{X}) = \delta_{allow} - \hat{g}(\mathbf{X}) \tag{6}$$

where  $\delta_{allow}$  values can be obtained from Table 1 for a specific performance level and  $\hat{g}(\mathbf{X})$  is the RS obtained from Section 3.4.





### 3.5.2 Strength LPFs

In the integrated reliability approach, the structural members are represented by beam-column elements. They are subjected to the combined effect of the axial load and bending moment. Considering the interaction effect, the equations suggested by AISC are used for the generation of the strength LPFs [12]. They can be represented as:

$$g(\mathbf{X}) = 1.0 - \left( \frac{P_u}{P_n} + \frac{8 M_{ux}}{9 M_{nx}} \right) = 1.0 - [\hat{g}_P(\mathbf{X}) + \hat{g}_M(\mathbf{X})]; \quad \text{if } \frac{P_u}{\phi P_n} \geq 0.2 \quad (7)$$

$$g(\mathbf{X}) = 1.0 - \left( \frac{P_u}{2P_n} + \frac{M_{ux}}{M_{nx}} \right) = 1.0 - [\hat{g}_P(\mathbf{X}) + \hat{g}_M(\mathbf{X})]; \quad \text{if } \frac{P_u}{\phi P_n} < 0.2 \quad (8)$$

where  $\phi$  is the resistance factor,  $P_u$  is the required compressive/tensile strength,  $P_n$  is the nominal compressive/tensile strength,  $M_{ux}$  is the required flexural strength, and  $M_{nx}$  is the nominal flexural strength. The functions  $\hat{g}_P(\mathbf{X})$  and  $\hat{g}_M(\mathbf{X})$  are RSs for the axial load and bending moment, respectively.  $P_n$  and  $M_{nx}$  can be determined using the AISC code [12]. The values of  $P_u/P_n$  are tracked in order to determine which interaction equation [Eq. (7) or (8)] is applicable for the reliability evaluation.

### 3.6 Calculation of structural reliability

The proposed algorithm appears to be complicated. For proper comprehension, it is summarized below. In the proposed algorithm, the necessary response information will be generated at the sampling points by calculating the maximum responses caused by an earthquake time history using SB-FEM. In the first iteration of FORM, an approximation of the LPF will be generated by using SD and Eq. (4) at the mean values of all RVs in the normal variable space. At the end of the first iteration, the sensitivity indexes of all RVs will be available. RVs with low sensitivity indexes will be considered as deterministic at their mean values and  $k$  will be reduced to  $k_r$ . The next iteration will start by using  $k_r$  number of RVs and a new LPF will be reconstructed using SD and Eq. (4). Using the updated LPF, the FORM iterations will continue until the RVs direction cosines converge to a pre-determined tolerance level [5]. Then, the first estimate of  $\beta$  will be calculated using the standard FORM procedure and the coordinates of the new checking point ( $x_i^*$ ) or center point will be recalculated as:

$$x_i^* = \mu_{x_i}^N - \alpha_i \beta \sigma_{x_i}^N \quad (9)$$

The overall updating will continue until  $\beta$  converges to a pre-established tolerance level [5]. In the context of the proposed ARS, in the final iteration, CCD and Eq. (5) will be used to generate a RS. Using the information on the required performance level, the corresponding LPF will be generated using the regression analysis. It usually takes 3 to 4 iterations to reach the convergence of the  $\beta$  value. Once  $\beta$  converged, the coordinates of the last checking point  $\mathbf{x}^*$ , representing the MPFP, will be calculated as:

$$\beta = \sqrt{(\mathbf{x}^*)^t (\mathbf{x}^*)} \quad (10)$$

Finally, based on the converged value of  $\beta$ , the corresponding  $p_f$  can be estimated as:

$$p_f = \Phi(-\beta) = 1.0 - \Phi(\beta) \quad (11)$$

A flowchart of the integrated structural reliability evaluation approach is shown in Fig. 1.

## 4. Incorporation of uncertainties in loads and resistance-related parameters

For the reliability estimation of real structures excited by the seismic loading in time domain, uncertainty associated with all major load and resistance-related parameters must be considered, as discussed below.

### 4.1 Uncertainties in resistance-related parameters

The uncertainties associated with resistance-related parameters are widely reported in the literature [5]. The appropriate information is used in this paper. The integrated approach will be demonstrated by considering the

performances of a steel building. All structural elements are represented by W-sections. Young’s modulus ( $E$ ), yield stress of columns ( $F_{yc}$ ) and girders ( $F_{yg}$ ), the cross sectional area ( $A$ ), and moment of inertia ( $I$ ) of W-sections used for structural elements are considered to be RVs with a lognormal distribution with Coefficient of Variations (COVs) of 0.06, 0.10, 0.10, 0.05, and 0.05, respectively, as shown in Table 2.

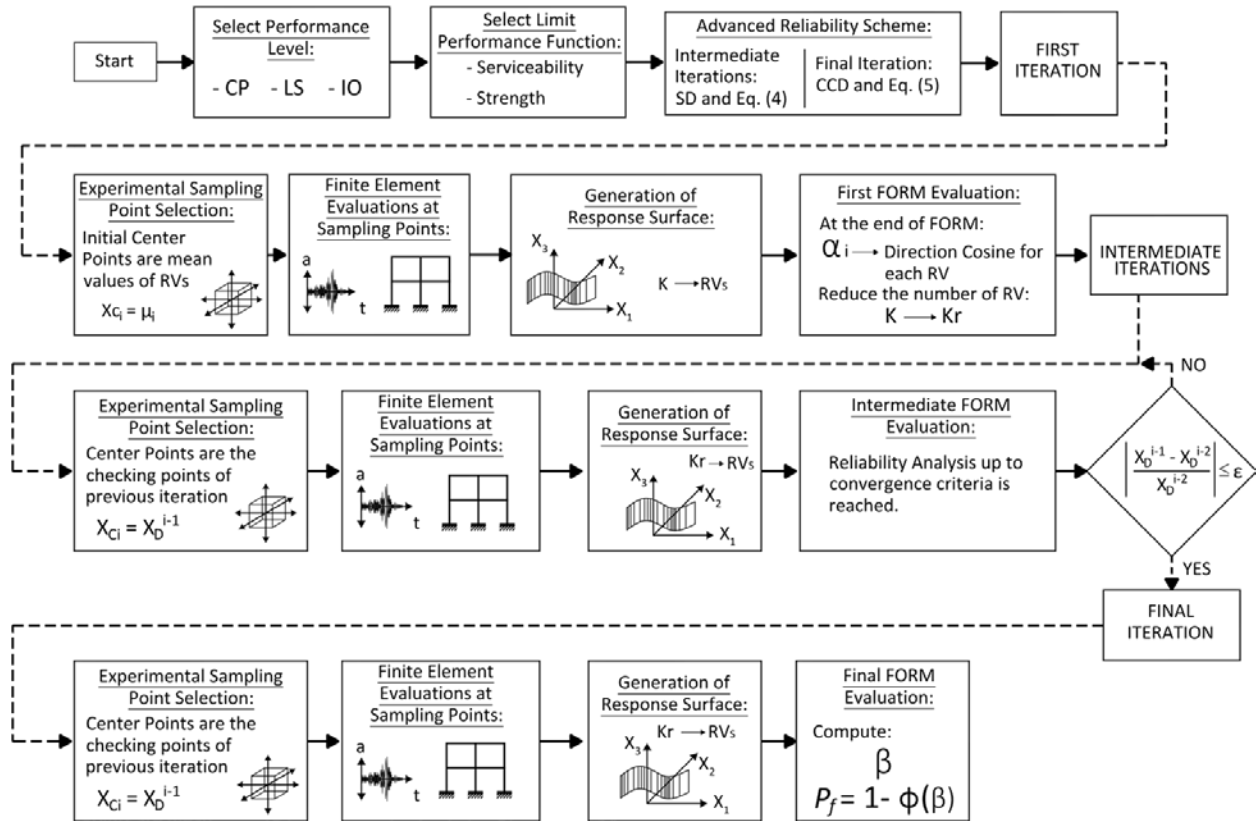


Fig. 1 – Flowchart of the integrated approach for PBS D

Table 2 – Uncertainties in resistance-related parameters, gravity loads, and seismic loading

Random Variable (RV)	Number of RVs	Distribution	Mean Value	COV
$E$ (kN/m <sup>2</sup> )	1	Lognormal	$1.9994 \times 10^8$	0.06
$F_{yc}$ * (kN/m <sup>2</sup> )	1	Lognormal	$3.4474 \times 10^5$	0.10
$F_{yg}$ ** (kN/m <sup>2</sup> )	1	Lognormal	$2.4822 \times 10^5$	0.10
$A$ (m <sup>2</sup> )	9	Lognormal	***	0.05
$I_x$ (m <sup>4</sup> )	9	Lognormal	***	0.05
$W_{D1}$ (kN/m)	1	Normal	32.9457	0.10
$W_{D2}$ (kN/m)	1	Normal	32.9457	0.10
$W_{L1}$ (kN/m)	1	Type 1	2.9188	0.25
$W_{L2}$ (kN/m)	1	Type 1	2.9188	0.25
$g_e$	1	Type 1	1.00	0.20

\*Yield stress of column sections (value reported in SAC).

\*\*Yield stress of girder sections (value reported in SAC).

\*\*\* A and  $I_x$  are considered as random variables for each section, however, their mean values are not reported. Following the standard practice, the information can be obtained in the AISC’s steel construction manuals [12]. The w-sections utilized for the analysis are given in Figure 2.



## 4.2 Uncertainties in gravity loads

In most design guidelines [13, 14], the gravity loads are classified as Dead Load (DL) and Live Load (LL). The uncertainties associated with both are available in the literature [5] and the authors used similar information in this paper. DL and LL are represented by a normal and Type 1 distributions with COV of 0.10 and 0.25, respectively, as shown in Table 2.  $W_{D1}$  and  $W_{D2}$  represent DL at the roof and floor levels, respectively.  $W_{L1}$  and  $W_{L2}$  are the LL for roof and floor levels, respectively. They will be discussed further later.

## 4.3 Uncertainties in seismic loading

As proposed here, for the PBSB guidelines, the seismic loading needs to be applied in time domain. Consideration of uncertainties in seismic loading is very challenging and the authors believe that it is still evolving. Uncertainty associated with the intensity and the frequency contents needs to be considered. In order to incorporate the uncertainty in the intensity, a factor ( $g_e$ ) is considered in this study. It is considered to be a RV with a Type 1 distribution and with a COV of 0.2 (see Table 2). To incorporate uncertainty in the frequency contents, several recent design guidelines [13, 14] suggested consideration of at least seven time histories expected for the location. For PBSB, multiple performance levels have to be considered and the corresponding risk or the probability of exceedance (PE) or reliabilities need to be estimated, as suggested by FEMA-273 [1] and SAC project [2-4]. Somerville et al. [15] developed three sets of ground motion time histories related to 2%, 10%, and 50% PE in 50 years for the Los Angeles (LA) area and correlated them with the performance levels of CP, LS, and IO, respectively. For every performance level, ten ground motions with two horizontal orthogonal components were proposed, providing twenty time histories per set. They applied Scale Factors (SFs) to match specific target response spectral values, on average, for periods at 0.3, 1.0, 2.0, and 4.0 seconds for site category  $S_D$  (firm soil), as suggested by the United States Geological Survey (USGS). Specific information on these earthquake (EQ) sets is summarized in Tables 3-5. The authors used these three sets of ground motions for the reliability evaluation of a 3-story steel frame.

Table 3 – Set 1: information and results for ground motions associated with 2% PE in 50 years and CP

EQ	Record Name	SF	PGA (g)	Excitation Time (sec)	LPF1		LPF2		LPF3		LPF4	
					$\beta$	TNSP	$\beta$	TNSP	$\beta$	TNSP	$\beta$	TNSP
1	1995 Kobe	1.15	1.282	25.0	7.5014	211	4.9755	211	1.9355	196	2.3275	226
2	1995 Kobe	1.15	0.920	25.0	5.4447	196	5.3499	211	3.9779	196	1.9441	211
3	1989 Loma Prieta	0.82	0.418	20.0	4.8429	226	5.9266	211	2.7789	196	4.2369	211
4	1989 Loma Prieta	0.82	0.473	20.0	5.4447	211	5.3499	211	2.7122	196	1.9441	211
5	1994 Northridge	1.29	0.868	14.0	7.7496	211	7.0797	211	3.3203	211	1.2765	211
6	1994 Northridge	1.29	0.943	14.0	10.1194	196	5.8313	226	2.6118	211	1.6330	196
7	1994 Northridge	1.61	0.926	15.0	3.8225	196	3.4900	196	2.9796	196	2.3302	211
8	1994 Northridge	1.61	1.329	15.0	5.0826	211	4.4267	196	1.3683	196	2.9744	226
9	1974 Tabas	1.08	0.808	25.0	6.0871	196	9.7849	211	3.0994	211	4.0253	211
10	1974 Tabas	1.08	0.991	25.0	4.2010	211	7.2582	211	3.3457	211	1.2503	196
11	Elysian Park (simulated)	1.43	1.295	18.0	6.6009	211	6.0138	226	2.8767	211	2.5854	226
12	Elysian Park (simulated)	1.43	1.186	18.0	5.5420	211	5.0964	226	2.6105	226	2.7017	211
13	Elysian Park (simulated)	0.97	0.782	18.0	6.5924	211	8.5152	211	3.2297	211	2.1669	196
14	Elysian Park (simulated)	0.97	0.680	18.0	4.1214	226	4.8303	211	3.0572	226	2.8329	226
15	Elysian Park (simulated)	1.1	0.991	18.0	10.6802	196	9.6892	211	3.8191	211	2.1858	196
16	Elysian Park (simulated)	1.1	1.100	18.0	4.3351	196	4.3612	211	2.0190	196	2.4040	211
17	Palos Verdes (simulated)	0.9	0.711	25.0	10.2074	211	10.1330	226	3.0781	211	2.3127	211





EQ	Record Name	SF	PGA (g)	Excitation Time (sec)	LPF1		LPF2		LPF3		LPF4	
					$\beta$	TNSP	$\beta$	TNSP	$\beta$	TNSP	$\beta$	TNSP
18	Palos Verdes (simulated)	0.9	0.776	25.0	6.3259	211	6.2217	196	3.3795	211	3.2340	211
19	Palos Verdes (simulated)	0.88	0.500	25.0	7.7473	211	10.6231	196	2.3450	211	3.6707	196
20	Palos Verdes (simulated)	0.88	0.625	25.0	6.6381	226	9.1280	211	3.3381	226	4.2738	211

Table 4 – Set 2: information and results for ground motions associated with 10% PE in 50 years and LS

EQ	Record Name	SF	PGA (g)	Excitation Time (sec)	LPF1		LPF2		LPF3		LPF4	
					$\beta$	TNSP	$\beta$	TNSP	$\beta$	TNSP	$\beta$	TNSP
21	Imperial Valley, 1940	2.01	0.461	25.0	4.8039	211	4.4713	196	3.4143	211	3.0675	211
22	Imperial Valley, 1940	2.01	0.675	25.0	4.4713	211	4.2363	196	3.7815	211	2.6002	211
23	Imperial Valley, 1979	1.01	0.393	15.0	5.1776	211	4.8687	211	2.2990	211	3.7083	211
24	Imperial Valley, 1979	1.01	0.488	15.0	8.4478	196	7.7164	211	4.0219	211	4.1048	211
25	Imperial Valley, 1979	0.84	0.301	15.0	10.6964	196	9.6924	226	2.9824	226	5.2702	211
26	Imperial Valley, 1979	0.84	0.234	15.0	5.6294	226	10.7162	196	5.3900	211	3.5289	196
27	Landers, 1992	3.2	0.421	30.0	7.2694	211	7.6101	211	4.8731	226	4.0915	196
28	Landers, 1992	3.2	0.425	30.0	6.7713	211	6.9528	226	5.3931	211	4.1856	211
29	Landers, 1992	2.17	0.519	30.0	5.8797	211	5.4032	211	2.7428	226	3.8440	196
30	Landers, 1992	2.17	0.360	30.0	5.6157	196	5.4589	226	5.2467	196	4.1749	211
31	Loma Prieta, 1989	1.79	0.665	16.0	5.6370	211	5.0078	196	2.1636	196	3.9029	211
32	Loma Prieta, 1989	1.79	0.969	16.0	4.6994	226	4.5689	211	3.8479	196	2.1463	196
33	Northridge, 1994, Newhall	1.03	0.678	15.0	5.7688	196	5.5237	226	4.0849	211	2.5029	226
34	Northridge, 1994, Newhall	1.03	0.657	15.0	4.3586	196	4.0475	211	4.3250	226	2.8114	211
35	Northridge, 1994, Rinaldi	0.79	0.533	14.0	6.7376	196	5.8265	211	4.6099	211	3.0637	226
36	Northridge, 1994, Rinaldi	0.79	0.579	14.0	5.5794	226	5.1310	211	0.1072	196	3.3381	211
37	Northridge, 1994, Sylmar	0.99	0.569	15.0	5.4197	211	6.1568	211	3.8668	226	3.8943	196
38	Northridge, 1994, Sylmar	0.99	0.817	15.0	4.1812	211	6.6290	196	3.1406	196	2.1686	226
39	North Palm Springs, 1986	2.97	1.018	16.0	5.5791	211	4.6285	226	2.8759	196	2.0495	211
40	North Palm Springs, 1986	2.97	0.986	16.0	7.7697	211	6.7888	226	4.1368	196	3.4581	226

Table 5 – Set 3: information and results for ground motions associated with 50% PE in 50 years and IO

EQ	Record Name	SF	PGA (g)	Excitation Time (sec)	LPF1		LPF2		LPF3		LPF4	
					$\beta$	TNSP	$\beta$	TNSP	$\beta$	TNSP	$\beta$	TNSP
41	Coyote Lake, 1979	2.28	0.589	12.0	7.5898	226	8.8855	196	4.4407	226	3.3547	211
42	Coyote Lake, 1979	2.28	0.333	12.0	5.2099	211	4.8470	196	7.7227	196	4.6268	211
43	Imperial Valley, 1979	0.4	0.143	15.0	8.9302	211	8.1173	211	5.7528	196	7.7608	211
44	Imperial Valley, 1979	0.4	0.112	15.0	9.6790	196	8.8961	211	3.1535	211	4.7703	211
45	Kern, 1952	2.92	0.144	30.0	9.3392	196	8.1685	211	7.5335	211	5.7477	196
46	Kern, 1952	2.92	0.159	30.0	4.2398	211	3.9089	211	7.7647	226	4.4785	211
47	Landers, 1992	2.63	0.337	25.0	3.5714	211	6.0831	211	5.9850	211	4.3143	226
48	Landers, 1992	2.63	0.307	25.0	4.6793	211	4.2649	196	4.2164	196	5.0059	226

EQ	Record Name	SF	PGA (g)	Excitation Time (sec)	LPF1		LPF2		LPF3		LPF4	
					$\beta$	TNSP	$\beta$	TNSP	$\beta$	TNSP	$\beta$	TNSP
49	Morgan Hill, 1984	2.35	0.318	20.0	3.9522	226	3.5836	226	1.4400	211	5.1498	226
50	Morgan Hill, 1984	2.35	0.546	20.0	4.3342	211	3.8307	226	2.5271	226	4.8230	211
51	Parkfield, 1966, Cholame	1.81	0.780	15.0	10.3906	211	7.7453	226	2.7651	211	3.0652	211
52	Parkfield, 1966, Cholame	1.81	0.631	15.0	9.1238	211	5.4750	211	4.3645	211	2.9714	211
53	Parkfield, 1966, Cholame	2.92	0.693	15.0	3.8215	211	3.2752	211	1.1809	211	4.2860	196
54	Parkfield, 1966, Cholame	2.92	0.790	15.0	7.6881	226	6.1587	211	4.6136	211	4.2777	196
55	North Palm Springs, 1986	2.75	0.517	20.0	4.2971	211	5.7535	196	3.6736	196	3.1593	196
56	North Palm Springs, 1986	2.75	0.379	20.0	4.1039	211	4.6217	196	6.8586	226	4.6564	211
57	San Fernando, 1971	1.3	0.253	20.0	4.6558	196	4.2702	211	7.1745	226	4.5004	196
58	San Fernando, 1971	1.3	0.231	20.0	7.0844	211	6.3298	211	8.2371	211	3.5474	211
59	Whittier, 1987	1.27	0.269	15.0	6.5021	226	8.1194	211	3.5638	211	3.8168	211
60	Whittier, 1987	1.27	0.167	15.0	7.9087	211	9.4006	211	5.0287	196	3.8022	196

### 5. Numerical example: reliability evaluation of a 3-story steel building

Several steel buildings were designed by experts during the SAC project. Among them, a 3-story steel building reported in FEMA-355C [3] is selected to demonstrate the application of the integrated approach. The building was specifically designed for the LA area, satisfying the post-Northridge earthquake requirements. A typical two dimensional frame representing the 3-story building and its respective W-sections for columns and girders are shown in Fig. 2.

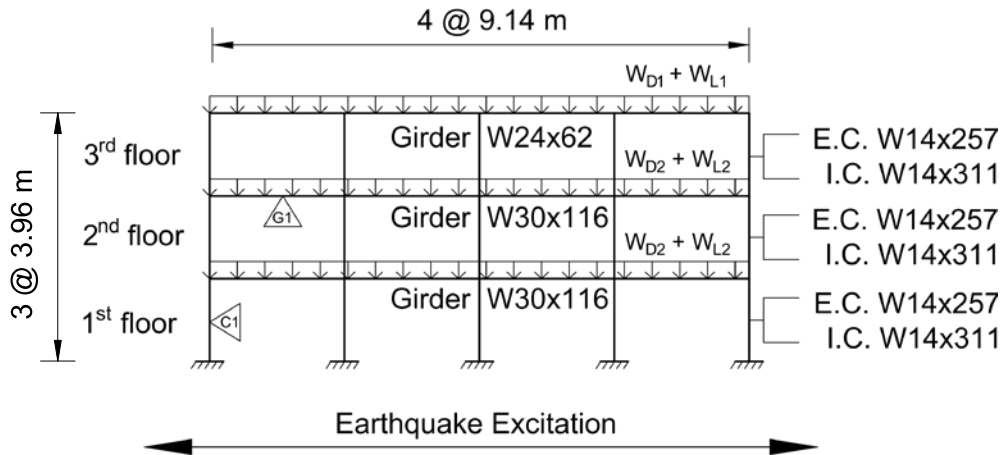


Fig. 2 – Two dimensional 3-story frame.

The frame is excited by every ground motion reported in Tables 3 to 5, and its structural reliability is calculated in terms of  $\beta$  considering four LPFs: overall top roof drift (LPF1), inter-story drift at the 2<sup>nd</sup> floor (LPF2), strength of column C1 (LPF3), and strength of girder G1 (LPF4). Column C1 and girder G1 are indicated in Fig. 2. Following the requirements summarized in Table 1, the corresponding  $\delta_{allow}$  for LPF1 are 59.4, 29.7, and 8.3 cm for CP, LS, and IO performance levels, respectively. The corresponding  $\delta_{allow}$  for LPF2 are 19.8, 9.9, and 2.8 cm, respectively. For LPF3 and LPF4, AISC interaction equations are used as explained earlier. The statistical information on all RVs is summarized in Table 2. For every LPF under consideration, the total number of RVs is 26, i.e.  $k = 26$ . Only 7 of them are found to be the most sensitive RVs or  $k_r = 7$ . The structural reliabilities are calculated for the three sets of ground motions representing three performance levels. Each set contains 10 earthquakes with two orthogonal components. The results of the reliability evaluations are summarized in Tables 3-5 in terms of  $\beta$  and TNSP for each LPF. It is observed that even for two components of



the same earthquake, the corresponding  $\beta$  values are different. This demonstrates that the design of a structure using only one earthquake time history is not adequate; several ground motions must be used, as recommended in recent building codes [13, 14]. The authors believe that this is a step in the right direction towards the development of PBSB guidelines.

The results in Tables 3 to 5 are summarized in Table 6 in terms of the mean reliability index ( $\bar{\beta}$ ) and the mean total number of sampling points ( $\overline{TNSP}$ ) for each set of ground motions and the LPF under consideration.

Table 6 – Mean values of  $\beta$  and  $TNSP$  per ground motion set and LPF

Probability of Exceedance	LPF1		LPF2		LPF3		LPF4	
	$\bar{\beta}$ ( $p_f$ )	$\overline{TNSP}$	$\bar{\beta}$ ( $p_f$ )	$\overline{TNSP}$	$\bar{\beta}$ ( $p_f$ )	$\overline{TNSP}$	$\bar{\beta}$ ( $p_f$ )	$\overline{TNSP}$
Set 1: 2% in 50 years (CP)	6.45 (5.5925e-11)	209	6.70 (1.0421e-11)	211	2.89 (0.0019)	208	2.62 (0.0044)	210
Set 2: 10% in 50 years (LS)	6.02 (8.7209e-10)	209	6.07 (6.3955e-10)	212	3.67 (1.2128e-04)	210	3.40 (3.3693e-04)	210
Set 3: 50% in 50 years (IO)	6.36 (1.0088e-10)	212	6.09 (5.6455e-10)	210	4.90 (4.7918e-07)	211	4.41 (5.1685e-06)	209

From the results presented in Table 6, it can be observed that  $\bar{\beta}$  for CP, LS, and IO corresponding to LPF1 are 6.45, 6.02, and 6.36, respectively. For LPF2, they are 6.70, 6.07, and 6.09, respectively. For the serviceability performance, the authors believe that the values suggested by FEMA-350 [2], as summarized in Table 1, are practical. The mean values of  $\beta$  for LPF1 and LPF2 are in the same range. They satisfy the basic intent of PBSB; i.e., the reliability should be similar for different performance functions. For the strength performance level and LPF3, the estimated  $\bar{\beta}$  values corresponding to CP, LS, and IO are 2.89, 3.67, and 4.90. For LPF4, they are 2.62, 3.40, and 4.41, respectively. Following the currently used Load and Resistance Factored Design (LRFD) guidelines, the mean  $\beta$  values for LS and IO appear to be acceptable. However, for CP, the  $\bar{\beta}$  values are below the acceptable level. The authors believe this is expected since the AISC’s interaction equations were proposed for the performance level of LS. The estimated reliability indexes correlate well with different levels of performance, as expected, indicating that the proposed reliability method is viable. The results and observations made in this study, clearly indicate that reliability information can be obtained using only few hundreds instead of several thousands or millions of deterministic analyses ( $TNSP$ ). The authors very strongly believe that the proposed reliability evaluation method can be used to advance the development of the PBSB concept.

## 6. Conclusions

The development of PBSB guidelines to be incorporated in the next generation design guidelines is a necessity and should be available as expeditiously as possible. Since PBSB is a risk-based concept, an appropriate risk evaluation procedure must be available to satisfy all the concerned parties. It must also satisfy the current design practices. To satisfy the deterministic design community, structures need to be represented by finite elements and the seismic loading must be applied in time domain. This will help to incorporate all major sources of nonlinearity and uncertainty in the formulation. However, for the class of problems under consideration, the required limit performance functions become implicit. Besides the basic MCS, the authors believe no other suitable reliability analysis procedure is currently available. A novel reliability evaluation procedure was proposed to fill this knowledge gap. The basic response surface method was significantly improved by removing its three major deficiencies and then it was integrated with the first-order reliability method to locate the failure region. In this way, an implicit limit performance function was approximately represented. Then, FORM was used to extract the reliability information. The authors developed required serviceability and strength LPFs and correlated them with the three performance levels of CP, LS, and IO, as suggested by FEMA and SAC. The proposed method was further illustrated with the help of an example. A 3-



story steel building was designed by experts satisfying post-Northridge design requirements, as reported by FEMA. The structure was excited by three sets of ground motions representing three performance levels of CP, LS, and IO. Each set contained 20 time histories representing one specific performance level. The results indicated that the structure is well-designed for the serviceability requirements as reported in FEMA-350. They are very similar to the values reported in the LRFD guidelines. For the strength LPFs, the authors assumed that the performance requirements for serviceability LPFs will also be applicable to strength LPFs. They used the interaction equations suggested by the AISC. The authors observed that the seismic design of structures needs to be performed by using several earthquake time histories, as suggested in some recent design guidelines. The reliability indexes estimated with the proposed method correlated well with different levels of performance, indicating that the proposed reliability method is viable. The results and observations made in this study clearly indicated that reliability information can be obtained using only few hundreds instead of several thousands or millions of deterministic analyses (TNSP).

## 7. Acknowledgements

This study is based on work partly supported by several agencies from the government of Mexico: *Consejo Nacional de Ciencia y Tecnología* (CONACYT), *Universidad Autónoma de Sinaloa* (UAS), and *Dirección General de Relaciones Internacionales de la Secretaría de Educación Pública* (DGRI-SEP). This study is also partially supported by the National Science Foundation under Grant No. CMMI-1403844. Any opinions, findings, conclusions, or recommendations expressed in this paper are those of the writers and do not necessarily reflect the views of the sponsors.

## 8. References

- [1] FEMA-273. NEHRP Guidelines for the Seismic Rehabilitation of Buildings: Federal Emergency Management Agency (FEMA), 1997.
- [2] FEMA-350. Recommended Seismic Design Criteria for New Steel Moment-Frame Buildings: Federal Emergency Management Agency (FEMA), 2000.
- [3] FEMA-355C. State of the Art Report on Systems Performance of Steel Moment Frames Subject to Earthquake Ground Shaking: Venture, SAC Joint. Federal Emergency Management Agency, 2000.
- [4] FEMA-355F. State of the Art Report on Performance Prediction and Evaluation of Steel Moment-Frame Buildings.: Venture, SAC Joint. Federal Emergency Management Agency, 2000.
- [5] Haldar A, Mahadevan S. Probability, reliability, and statistical methods in engineering design: John Wiley & Sons, Incorporated, 2000.
- [6] Kondoh K, Atluri S. Large-deformation, elasto-plastic analysis of frames under nonconservative loading, using explicitly derived tangent stiffnesses based on assumed stresses. *Comput Mech* 1987;2:1-25.
- [7] Gao L, Haldar A. Nonlinear Seismic Analysis of Space Structures with Partially Restrained Connections. *Computer-Aided Civil and Infrastructure Engineering* 1995;10:27-37.
- [8] Reyes-Salazar A, Haldar A. Nonlinear seismic response of steel structures with semi-rigid and composite connections. *Journal of Constructional Steel Research* 1999;51:37-59.
- [9] Huh J, Haldar A. Stochastic finite-element-based seismic risk of nonlinear structures. *J Struct Eng* 2001;127:323-9.
- [10] Mehrabian A, Haldar A, Reyes-Salazar A. Seismic response analysis of steel frames with post-Northridge connection. *Steel and Composite Structures* 2005;5:271-87.



- [11] Khuri AI, Cornell JA. Response surfaces: designs and analyses: CRC press, 1996.
- [12] AISC. Steel Construction Manual, Chicago, Illinois 60601-1802: American Institute of Steel Construction, 2011.
- [13] ASCE/SEI 7-10. Minimum Design Loads for Buildings and Other Structures. American Society of Civil Engineers, Reston, Virginia 20191: ASCE, 2010.
- [14] IBC I. International Code Council. International Building Code. International Code Council: Washington DC, United States 2012.
- [15] Somerville PG, Venture SJ. Development of ground motion time histories for phase 2 of the FEMA/SAC steel project: SAC Joint Venture, 1997.